
This is an electronic reprint of the original article.
This reprint may differ from the original in pagination and typographic detail.

Ghazalian, Reza; Golipoor, Sahar

A Study on the Effect of Phase Shifter Quantization Error on the Spectral Efficiency Using Neural Network

Published in:

Proceedings - 2022 IEEE 4th Global Power, Energy and Communication Conference, GPECOM 2022

DOI:

[10.1109/GPECOM55404.2022.9815775](https://doi.org/10.1109/GPECOM55404.2022.9815775)

Published: 11/07/2022

Document Version

Peer reviewed version

Please cite the original version:

Ghazalian, R., & Golipoor, S. (2022). A Study on the Effect of Phase Shifter Quantization Error on the Spectral Efficiency Using Neural Network. In *Proceedings - 2022 IEEE 4th Global Power, Energy and Communication Conference, GPECOM 2022* (pp. 626-631). (Proceedings - 2022 IEEE 4th Global Power, Energy and Communication Conference, GPECOM 2022). IEEE. <https://doi.org/10.1109/GPECOM55404.2022.9815775>

This material is protected by copyright and other intellectual property rights, and duplication or sale of all or part of any of the repository collections is not permitted, except that material may be duplicated by you for your research use or educational purposes in electronic or print form. You must obtain permission for any other use. Electronic or print copies may not be offered, whether for sale or otherwise to anyone who is not an authorised user.

A Study on the Effect of Phase Shifter Quantization Error on the Spectral Efficiency Using Neural Network

Reza Ghazalian and Sahar Golipoor

Department of Communications and Networking, Aalto University

Email: reza.ghazalian@aalto.fi

Abstract—Beamforming (BF) is the inevitable component of the recent communication systems, especially Millimeter wave (mmWave) systems. Thanks to the radio frequency (RF) and digital technologies, BF techniques are implemented in the both digital and analogue domains by using phase shifters (PS) networks. Adopting the digital PS, which has the finite resolution bits, leads to loss in the spectral efficiency (SE). Accordingly, in this paper, we extract the SE loss in a multi-user multiple inputs single output (MISO) system, which would be useful for practical prospective. To this end, we apply machine learning (ML) to extract the SE loss. Simulation results show that the extracted models have the desirable accuracy in the SE loss prediction.

Index Terms—Phase shifter resolution bits, Spectral efficiency loss model, Neural Networks.

I. INTRODUCTION

Beamforming (BF) techniques play an important role in all communication and sensing systems. These are usually implemented with phase shifters (PS) network with constant amplitude constraint [1]. One of the implementation ways of the PSs is using digital technology with N_b -bit resolution discrete phase [1], [2]. The important specification of these PSs, which concern a system designer, is quantization error. Reduction in the PS quantization error would result in an increase in the cost of PS. Trading off the cost and system performance would be critical in the Millimeter wave (mm-Wave) systems, where a huge number of PSs (from a few hundred to several thousand) are used [3]. Meanwhile, spectral efficiency (SE) is one of the important metrics for the evaluation of system performance. Therefore as a practical aspect, a system designer would like to have insight to how the PS quantization error degrades SE, especially for communication and sensing scenarios [4] and even for wireless power transfers device connectivity [5].

There are some researches conducted on the effect of PS error on the SE degradation [1], [2], [6], [7]. The loss of the achievable rate with root-mean-square (RMS) phase error and RMS gain error investigated in the multi-stream point to point multiple inputs multiple outputs (MIMO) scenario and multi-user massive MIMO scenario in the mm-Wave communication system [2]. The achievable rate degradation also derived in a closed form for point to point multi-user massive MIMO as a result of using PS quantization error [6], [7].

Basically, we are interested in increasing SE. So we should deal with SE loss. Needless to say, we first need to pre-

dict SE loss and then design algorithms to compensate this degradation. To the best of our knowledge, there are some parameters play roles in the SE loss as the results of using low resolution digital PS such as the angular distances between users, which have been rarely addressed in the literature. We will investigate these influential parameters in this paper. The relationship between these parameters and SE loss is a complicated function that cannot be derived in a closed form. In these cases, ML techniques are helpful in prediction. All the above matters motivated us to focus on extracting the SE loss model based on the ML techniques in this paper. Accordingly, the main contributions of this paper are: 1) In the down-link multi-user multiple inputs single output (MISO) communications system, we extract the SE loss due to a finite resolution PS (SEFRPS) by using neural networks (NN); 2) To obtain the SE loss, we examine some influential parameters on the SE such as: the number of AP's antennas, the number of users, the antenna's surface angle with respect to the x axis (ASA) of the AP, the power budget at the AP, and the angular distances between a pair users. Thus, based on these parameters as well as the number of PS's bits, we build database through the Monte-Carlo simulation.

The rest of the paper is organized as follows. In Section II, the system model as well as the channel model are described. In Section III, we study the effect of some parameters on the SEFRPS and describe the ML model. Simulation results are shown in Section IV to validate the SEFRPS model. Finally, the conclusion is presented in Section V.

Notations: Boldface lowercase letters denote column vectors, \mathbf{x} . $X_{i,j}$ is the i th row j th column element of matrix \mathbf{X} and $\mathbf{X}_{:,j}$ is the j th column of matrix \mathbf{X} . \mathbf{I} denotes the identity matrix, and $\mathbf{diag}(\mathbf{x})$ is a diagonal matrix with the main diagonal from entries of \mathbf{x} . $(\cdot)^T$, $(\cdot)^H$, and $\angle(\cdot)$ denote the transpose, Hermitian transpose, and angle value operations, respectively. \mathbb{C} is the set of complex numbers. In addition, $\mathbb{CN}(0, N_0)$ is a circularly-symmetric complex Gaussian random variable with zero mean and variance value N_0 . N_0 also shows the spectral density of the noise.

II. SYSTEM MODEL

A. System Model

In this paper, we have considered a down-link scenario where a AP equipped with N_{AP} antennas serves N_{user}

single-antenna users simultaneously ($N_{AP} \geq N_{user}$). The topology of the considered network is shown in Figure 1. U_{AZ} demonstrates the angular distance between two adjacent users viewed from the AP. It is also assumed that all users have the same distances from the AP, i.e. d . This assumption has been taken to ignore the effect of the distance in the path loss component for all users.

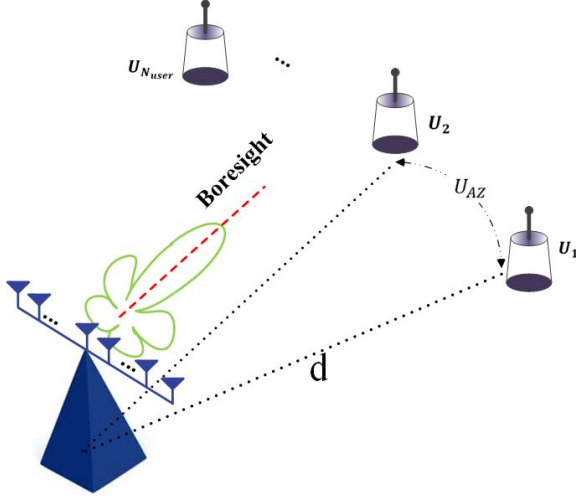


Fig. 1: The topology of the considered scenario

Further, we assume that the AP implements the zero forcing beam forming (ZFBF) in the radio frequency (RF) domain via the digital PS network, and the number of RF chain is equal to the number of users, $N_{user} = N_{RF}$. N_{RF} shows the number of RF chains, which contain PS. Moreover, the knowledge of the channel state information (CSI) is assumed to be perfect at the AP. Besides, the symbol vector $\mathbf{s} \in \mathbb{C}^{N_{user} \times 1}$ where $E[\mathbf{s}\mathbf{s}^H] = \mathbf{I}_{N_{user}}$ is precoded by the analogue precoder $\mathbf{W} \in \mathbb{C}^{N_{AP} \times N_{user}}$ at the AP. Indeed, we have used fully connected PS network for the analogue BF (ABF) implementation such that the elements of the ABF matrix are limited to the constant amplitude constraint. Then, the transmitted signal vector denoted as \mathbf{x} can be written as

$$\mathbf{x} = \mathbf{W}\mathbf{s}. \quad (1)$$

The i th row and the j th element of ABF matrix (\mathbf{W}) can be written as

$$[W]_{i,j} = e^{j\theta_{i,j}}, \quad (2)$$

where $\forall \theta_{i,j} \in \Theta, i \in \{1, \dots, N_{AP}\}, j \in \{1, \dots, N_{user}\}$ and $\Theta = [0, \frac{2\pi}{2N_b}, \dots, (2N_b - 1)\frac{2\pi}{2}]$ and N_b shows the number of bits of the PS.

Based on the considered scenario, the received signal at the k th user can be modeled as:

$$y_k = \underbrace{\sqrt{p_k} \mathbf{h}_k \mathbf{W}_{:k}}_{\text{desired signal}} s_k + \underbrace{\sum_{j=1, j \neq k}^{N_{user}} \sqrt{p_j} \mathbf{h}_j \mathbf{W}_{:j}}_{\text{interference signal}} s_j + z_k, \quad (3)$$

where p_k shows the allocated power at AP to the k th user, $\mathbf{h}_k \in \mathbb{C}^{1 \times N_{AP}}$ denotes the channel vector from the AP to the k th user, which will be described later and $z_k \sim \mathbb{CN}(0, N_0)$ is the received noise signal with the independent and identically distributed (i.i.d.) at the k th user.

B. Channel Model

In this paper, we assume that AP is equipped with a uniform linear array (ULA). We also presume that the channel between the AP and the k th user is modelled by Rayleigh fading channel as [8], [9]:

$$\mathbf{h}_k = \sqrt{\frac{N_{AP}\mathbb{L}}{M_p}} \sum_{m=1}^{M_p} \gamma_{k,m} \mathbf{a}_{AP}(\phi_{k,m}), \quad (4)$$

where $\gamma_{k,m} \sim \mathbb{CN}(0, 1)$ shows the path coefficient of the m th scattering path corresponding to the k th user. M_p is the total number of scattering path, which is assumed to be one for the sake of simplification. $\phi_{k,m}$ represents the angle of departure at the AP for the m th scattering path. Besides, \mathbb{L} is the distance dependent path loss model which can be written as :

$$\mathbb{L} = L_0 \left(\frac{d}{d_0}\right)^{-\alpha}, \quad (5)$$

where L_0 denotes the path loss at the reference distance $d_0 = 1$ meter, α is the path loss exponent. In addition, $\mathbf{a}_{AP}(\cdot)$ shows the antenna array response at the AP. Thus, the N_{AP} -dimensional antenna array response vector at angle ϕ , for ULA structure is modeled as [10]:

$$\mathbf{a}_{AP}(\phi) = \frac{1}{N_{AP}} (1, \nu^1, \dots, \nu^{2N_{AP}-1})^T, \quad (6)$$

where $\nu = e^{-j\frac{2\pi d_{as}}{\lambda} \cos(\phi)}$, λ is the wavelength of the carrier frequency and $d_{as} = \frac{\lambda}{2}$ is the antenna spacing [10].

III. THE METHODOLOGY

To extract SELFRPS, we use the regression ML model with the aid of neural network. Firstly, some influential factors on the SELFRPS are described, which are as the inputs of the ML model. Then, the structure of the considered NN is explained. Note that the ML model proposed in this paper is just one of the possible solutions for the SELFRPS function extraction. Besides, the ML model is trained in an offline manner.

A. Influential factors on SELFRPS

Based on our simulation and considering the BF techniques in multi-user scenarios, there are some influential factors on the SELFRPS. The following subsections describe these important factors. Indeed, based on their effects on the SE loss, we define them as the inputs of the ML model.

1) **PS bits resolution:** To show the effect of the PS bits resolution, first, we briefly explain how the digital PS applies the phase shifting. Regarding ZFBF, \mathbf{W} is modeled as:

$$\mathbf{W} = \mathbf{H}^\dagger \Lambda^{\frac{1}{2}} \mathbf{G}^{\frac{1}{2}}, \quad (7)$$

where $\mathbf{H}^\dagger = \mathbf{H}^H (\mathbf{H}\mathbf{H}^H)^{-1}$ shows Moore-Penrose (right) pseudo-inverse of \mathbf{H} , $\mathbf{H} = [\mathbf{h}_1^T, \mathbf{h}_2^T, \dots, \mathbf{h}_{N_{user}}^T]^T$.

The column-normalizing diagonal matrix $\Lambda = \mathbf{diag}(\alpha_1, \alpha_2, \dots, \alpha_{N_{user}})$ contains the reciprocal of the squared norm of the columns of \mathbf{H}^\dagger on the diagonal. $\mathbf{G} = \mathbf{diag}(g_1, g_2, \dots, g_{N_{user}})$ is a diagonal matrix which shows the assigned power to the users. The quantization phase of $W_{i,j}$, i.e. $Q(\angle W_{i,j})$, is also applied. $Q(\cdot)$ shows the quantization function and maps each angle of $W_{i,j}$ into the nearest phase value in the set Θ .

To calculate the SE, the water-filling power allocation is applied [11]. Based on that, the SELFRPS is the difference between the ideal achievable SE and the non-ideal one. Note that the ideal achievable SE and the non-ideal one are obtained by using PA method with the infinite resolution PS and the N_b resolution PS, respectively. Figure 2 shows the SELFRPS in terms of N_b . As can be seen, as the resolution of the PS increases, the SELFRPS decreases. Of course, the SELFRPS dose depend on the scenario. In fact, changing some factors like the AP's array antenna size and the number of users can alter the effect of N_b on the SE loss.

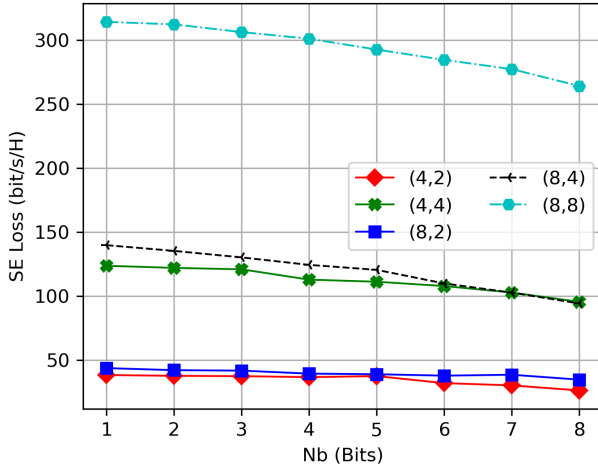


Fig. 2: The effect of N_b on the SE loss in terms of (N_{AP}, N_{user}) for $U_{AZ} = 2^\circ$, $P_t = 30$ dBm, and $\theta_A = 0^\circ$

On top of that, as can be seen in Figure 3, the PS resolution also affects on the beam-pattern of the array antenna. Figure 3 has been extracted based on the scenario in which $N_{AP} = 8$ and $N_{user} = 3$ and the first user are located in the direction $\theta = 0^\circ$ towards to the AP. The angular distance between the two users is assumed to be 10° . Note, Figure 3 shows the beam pattern of the first user and the ideal beam pattern is shown by black line. The ideal beam pattern is obtained by using the infinite resolution PS. As can be observed, there is a null beam in the direction $\theta = 0^\circ$ towards the user when using 2-bit PS; whereas, the main lobe of the ideal beam pattern is exactly there. Hence, using 2-bit resolution PS in this scenario leads to the dramatic SE loss which has seen in Figure 2 as well. Moreover, Figure 3 shows that, as the PS resolution increases, the beam pattern of the array antenna goes closer to the ideal one.

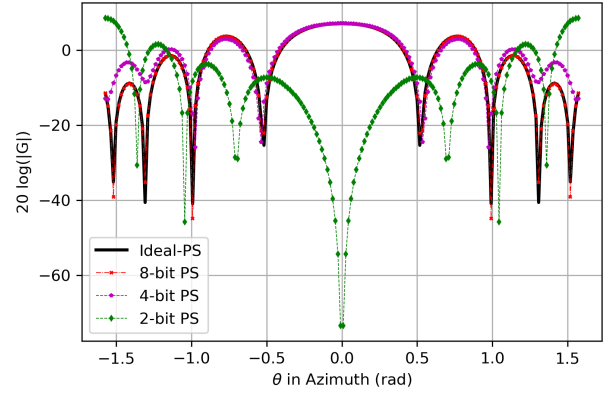


Fig. 3: The effect of N_b on the array antennas beam pattern

2) *The number of AP's array antennas and the number of Users:* Refer to Figure 2, the more the number of AP's antennas, the more loss in SE. The reason is definitely aggregation of the phase quantization error. In addition, growing the number of users increases the SE loss (see the Figure 2). To explain the reason, consider Figure 3. As can be seen, using a low resolution PS leads to change the main lobe level as well as the location of the null beam from the ideal one. This not only decreases the desired signals level, but it also increases the interference signals. This degrades the SE of the system. In this case, it is clear that the SE degradation rises as the number of the users increases.

3) *The total power at the AP:* As Figure 4 demonstrates, the power budget at the AP is the another influential factor on the SELFRPS. The more power budget increases at the AP, the more the SE loss increases. Moreover, as the PS's bits declines, the effect of the AP's power budget on the SELFRPS is intensified. For clarification, consider 2-bit PS and its main and side lobe levels in Figure 3. It can be realized that increasing the transmitted power at the AP not only cannot help the system to enhance the desired received signals, but also strengthens the interference levels. Indeed, using the low resolution PS shifts the main lobe of the beam pattern from its desired location. Therefore, the desired signal at the user attenuates. Furthermore, increase in the null beam level intensifies the interference level at the user side. Consequently, the SINR at the user decreases, which results in the SE loss. This analysis can be extended for the other N_b -bit digital PS.

4) *The angular distances among Users and the ASA of the AP:* The users' angular distance (i.e., angular separations between two adjacent users) and the ASA of the AP have simultaneously effects on the SE loss. To show their effects, we extract the SELFRPS as the two dimensional function of the AP's ASA and the users' angular distance, which is shown in Figure 5. As can be seen, even for the determined resolution of the PS, SE loss changes with respect to the value of the AP's ASA and the users' angular distance.

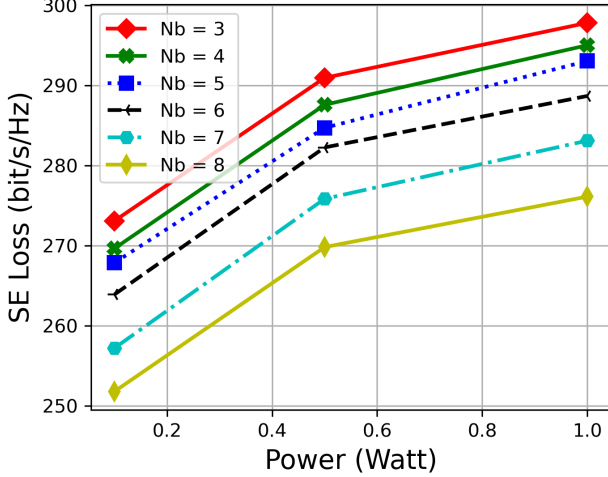


Fig. 4: The effect of power budget at the AP on the SE loss for $N_{AP} = 8$, $N_{user} = 4$, $U_{AZ} = 2^\circ$, and $\theta_A = 0^\circ$

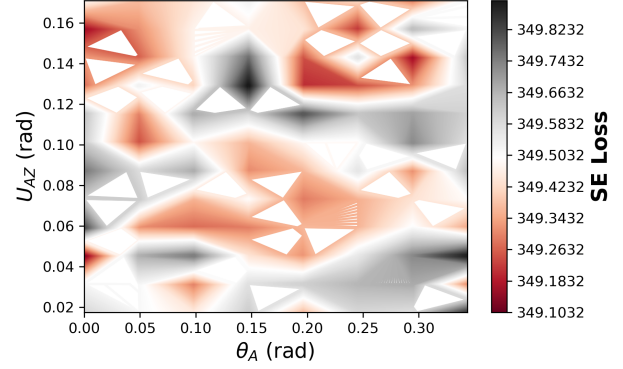
B. The ML model

In this paper, we adopt a fully-connected neural network with rectifier linear units (ReLU) activation function as shown in Figure 6. Since there is not any proper database to extract SELFRPS model based on NN, we obtain database through the Monte Carlo simulation to train NN. To this end, the aforementioned factors including the number of PS bits (N_b), the number of AP's array antennas (N_{AP}), the number of users (N_{user}), the power budget at the AP (P_t), the user's angular distance in azimuth (U_{AZ}), and the ASA of the AP (θ_A) are considered as the inputs of the NN. In fact, they are features for the regression problem. Generally, the input vector of the NN is defined as:

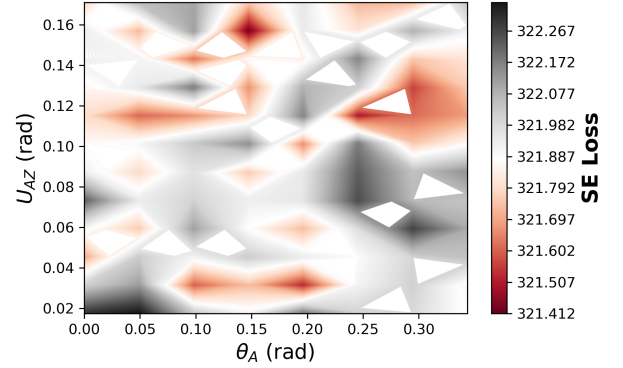
$$\psi = [N_{AP}, N_{user}, U_{AZ}, N_b, P_t, \theta_A]^T. \quad (8)$$

Moreover, the SELFRPS, $\widehat{\Delta SE}$, has been taken into account as the output of the NN.

Database: We define $N_{AP} \in \{4, 8\}$, $N_{user} \in \begin{cases} 1, 2, 3, 4 & N_{AP} = 4 \\ 1, 2, \dots, 7, 8 & N_{AP} = 8 \end{cases}$, $U_{AZ} \in \{2^\circ, 6^\circ, 4^\circ, 8^\circ\}$, $N_b \in \{1, 2, \dots, 8\}$, $P_t \in \{0.2, 0.4, 0.6, 0.8, 1\}$ Watts, and $\theta_A \in \{0^\circ, 25^\circ, 50^\circ, 75^\circ\}$. Since these data points are so scattered, we normalize them to one in order to achieve a better accuracy for the SELFRPS prediction. In addition, for each state, e.g. $\psi = [4, 3, 2^\circ, 2, 1, 0^\circ]^T$, we generate and save 1000 realizations of the stochastic Rayleigh channels described before. Thus, we obtain the database with the length of 1920000. After that, for each channel realization, the ZFBF technique combined with the water-filling PA method are adopted to calculate the SELFRPS. The SELFRPS is the difference value of the ideal SE and the non-ideal SE. Note that the ideal SE and the non-ideal SE are obtained through the PA along with ZFBF when the infinite resolution PS and the limited resolution PS are used, respectively. These obtained SELFRPSes are labeled



(a)



(b)

Fig. 5: The effect of the angular distances among users and the ASA of AP on the SELFRPS for, $N_{AP} = 8$, $N_{user} = 8$, $P_t = 30$ dBm: (a) 4-bit Digital PS; (b) 7-bit Digital PS.

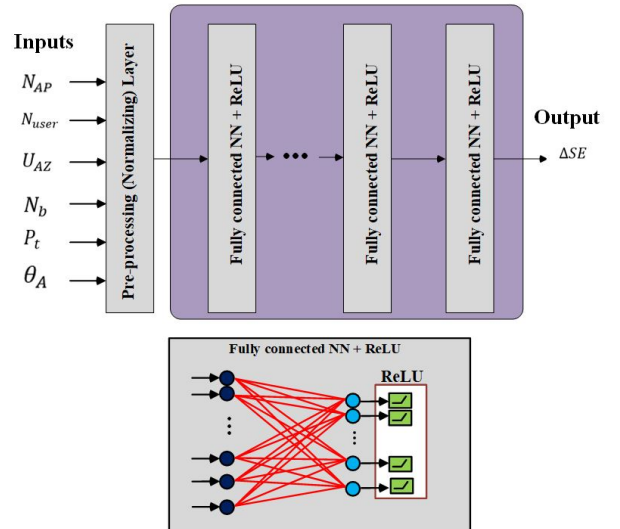


Fig. 6: The Structure of the considered NN

as the outputs for the ML training phase corresponding to their inputs.

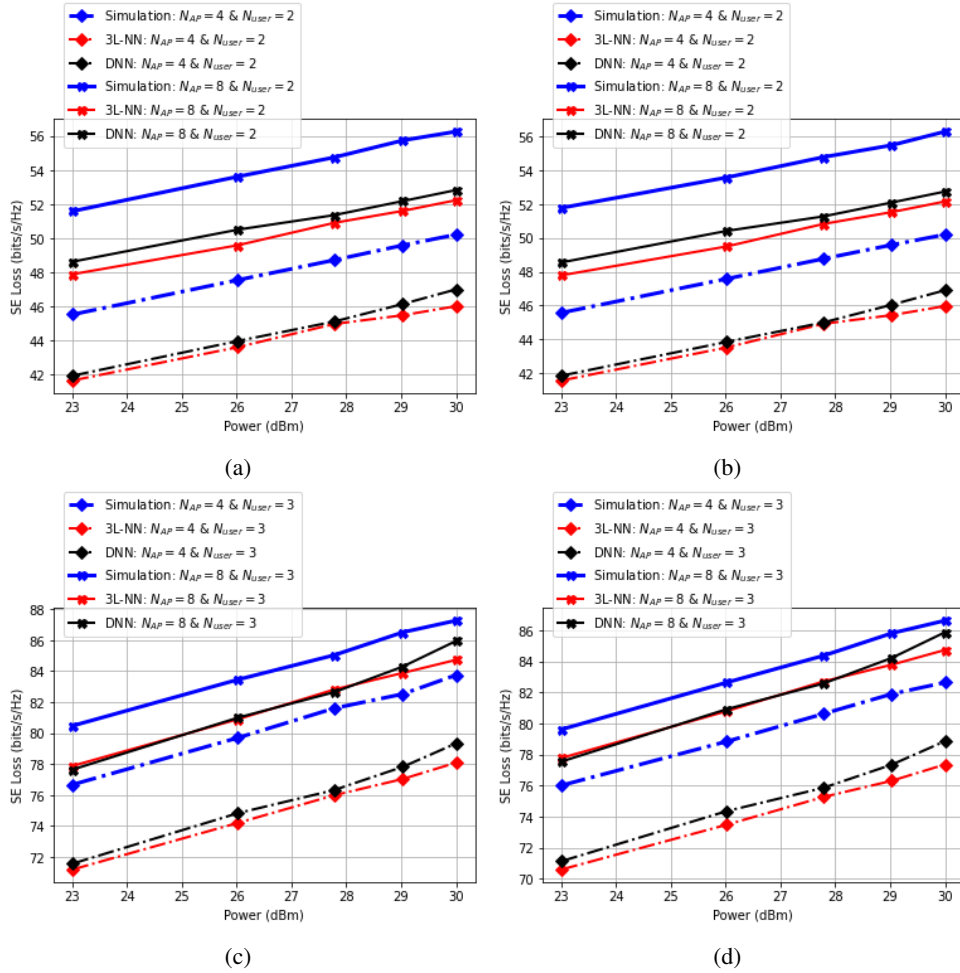


Fig. 7: Comparison of the predicted SELFRPS obtained through DD-NN, 3L-NN and simulation: (a) $N_b = 2\text{bits}$, $U_{AZ} = 8^\circ$, $\theta_A = 0^\circ$; (b) $N_b = 4\text{bits}$, $U_{AZ} = 8^\circ$, $\theta_A = 0^\circ$; (c) $N_b = 2\text{bits}$, $U_{AZ} = 8^\circ$, $\theta_A = 0^\circ$; (d) $N_b = 4\text{bits}$, $U_{AZ} = 8^\circ$, $\theta_A = 0^\circ$.

Loss function: The considered NN aims to predict SELFRPS as the function of ψ . The NN is trained to make ΔSE , the labeled SELFRPS, as close as possible to $\widehat{\Delta SE}$. Accordingly, the NN is trained to minimize the loss function, $\mathcal{L}_{NN}(\psi)$, defined as:

$$\mathcal{L}_{NN}(\psi) = \frac{1}{n_{tr}} \sum_{i=1}^{n_{tr}} (\Delta SE_i - \widehat{\Delta SE}_i)^2, \quad (9)$$

where n_{tr} is the number of training data set. We dedicate 70% of the total database for the NN training phase, and 30% of the database for the validation phase. Noting that the training data are randomly shuffled at each epoch.

IV. THE SIMULATION RESULTS

In this section, we evaluate the performance of the extracted SELFRPS model. To do so, we compare it with the SELFRPS obtained via the simulation. We set the scenario and average the SELFRPS obtained by the methods over 2000 independent fading channel realizations, with $L_0 = 20\text{dB}$, $\alpha = 2$, and $N_0 = -110\text{dBm}$. In addition, it is assumed that all users have the same distance from the AP with $d = 20$ meters.

We train two fully connected NNs with 3 layers and 7 layers, which are respectively called 3 layers NN (3L-NN) and Deep layer NN (DNN). In the both NNs, the activation function is assumed to be ReLU. The number of neurons in the hidden layers of the 3L-NN are respectively 100, 80, 40. For the DNN, there are respectively 80, 60, 60, 60, 60, 60, 10 neurons in the hidden layers.

The value of the SELFRPS obtained by the considered NNs are compared with the results achieved through the simulation to show their accuracy in the SELFRPS prediction. The accuracy of the predicted SELFRPS of the NNs is shown in Figure 7. To draw more insight for the accuracy of the extracted models, the simulations are conducted for different parameters. As can be seen, as the power budget at the AP increases, the accuracy of the both NNs increases, especially in a scenario with the AP equipped with the larger array antenna size. The figures demonstrate that the DNN has the better accuracy than that of the 3L-NN. However, the accuracy rate of the 3L-NN approaches to the DNN accuracy by rising the number of AP array antennas when $N_{user} = 3$. Overall, the both NN models have the accuracy rate between of 90% to 98%, approximately.

It should be mentioned that 3L-NN outperforms the DNN in terms of the computational complexity. On top of that, it can be reached to a better performance by using other ML methods and suitably adjusting their parameters, which would be interesting for the future research direction.

V. CONCLUSION

In this paper, we have investigated the impact of the finite resolution PS on the SE loss. By conducting some simulations, we have shown that there are some other factors influenced on the SE loss. Furthermore, we have extracted the SE loss as the multidimensional function of the influential factors by leveraging the fully connected NN. To demonstrate the impact of the NN design, we have compared two NNs with the different hidden layers and nodes. Simulation results have been revealed that the deeper NN has the better accuracy than the another one in the SE loss prediction. Besides, the accuracy rate of the extracted NNs are between of 90% to 98%. Using other ML methods and considering more factors as inputs, the results would be better.

ACKNOWLEDGMENT

This work has been funded in part by Academy of Finland ULTRA (n:o 328215) project.

REFERENCES

- [1] W. Wang, H. Yin, X. Chen, and W. Wang, "Robust and low-overhead hybrid beamforming design with imperfect phase shifters in multi-user millimeter wave systems," *IEEE Access*, vol. 8, pp. 74 002–74 014, 2020.
- [2] W. Wang, H. Yin, X. Chen, and W. Wang, "Performance loss of hybrid beamforming with imperfect phase shifters in millimeter wave systems," in *2018 IEEE 88th Vehicular Technology Conference (VTC-Fall)*.
- [3] W. Tan, D. Xie, J. Xia, W. Tan, L. Fan, and S. Jin, "Spectral and energy efficiency of massive MIMO for hybrid architectures based on phase shifters," *IEEE Access*, vol. 6, pp. 11 751–11 759, 2018.
- [4] M. A. Islam, G. C. Alexandropoulos, and B. Smida, "Integrated sensing and communication with millimeter wave full duplex hybrid beamforming," *arXiv preprint arXiv:2201.05240*, 2022.
- [5] S. Golipour, S. M. Andargoli, and R. Ghazalian, "A low complexity power allocations algorithm for DF MIMO SWIPT relaying systems," *Internet Technology Letters*, vol. 4, no. 2, p. e213, 2021.
- [6] S. Payami, M. Ghoraiishi, and M. Dianati, "Hybrid beamforming for large antenna arrays with phase shifter selection," *IEEE Transactions on Wireless Communications*, vol. 15, no. 11, pp. 7258–7271, 2016.
- [7] L. Zhao, D. W. K. Ng, and J. Yuan, "Multi-user precoding and channel estimation for hybrid millimeter wave systems," *IEEE Journal on Selected Areas in Communications*, vol. 35, no. 7, pp. 1576–1590, 2017.
- [8] O. El Ayach, S. Rajagopal, S. Abu-Surra, Z. Pi, and R. W. Heath, "Spatially sparse precoding in millimeter wave MIMO systems," *IEEE transactions on wireless communications*, vol. 13, no. 3, pp. 1499–1513, 2014.
- [9] X. Gao, L. Dai, S. Han, I. Chih-Lin, and R. W. Heath, "Energy-efficient hybrid analog and digital precoding for mmwave MIMO systems with large antenna arrays," *IEEE Journal on Selected Areas in Communications*, vol. 34, no. 4, pp. 998–1009, 2016.
- [10] D. Tse and P. Viswanath, *Fundamentals of wireless communication*. Cambridge university press, 2005.
- [11] T. Yoo and A. Goldsmith, "On the optimality of multiantenna broadcast scheduling using zero-forcing beamforming," *IEEE Journal on selected areas in communications*, vol. 24, no. 3, pp. 528–541, 2006.